PHYSICAL REVIEW B **76**, 180408(R) (2007)

Direct observation of rare-earth-host interactions in $Er:Y_2SiO_5$

O. Guillot-Noël,[1,*] H. Vezin,[2] Ph. Goldner,[1] F. Beaudoux,[1] J. Vincent,[1] J. Lejay,[1] and I. Lorgeré[3]
[1]*Ecole Nationale Supérieure de Chimie de Paris (ENSCP), Laboratoire de Chimie de la Matière Condensée de Paris, CNRS-UMR 7574, ENSCP, 11 rue Pierre et Marie Curie 75231 Paris Cedex 05, France*
[2]*Laboratoire de Chimie Organique et Macromoléculaire, CNRS UMR 8009, Bat C4, F-59655 Villeneuve d'Ascq Cedex, France*
[3]*Laboratoire Aimé Cotton, CNRS-UPR 3321, Bât. 505, 91405 Orsay Cedex, France*
(Received 6 November 2007; published 30 November 2007)

We report the direct observation of Er-Y and Er-Si interactions in $Er:Y_2SiO_5$ by spin-echo measurements. Modulations in the spin-echo decay of Er^{3+} ions are due to magnetic interactions between the rare earth and the host nuclear spins. The closest yttrium ions were found to be out of resonance compared to the yttrium ions farther away from the rare earth. This strong "frozen core" effect around the Er^{3+} ions suggests that the influence of Y^{3+} ions on the decoherence processes of erbium is weaker than what can be deduced from the yttrium in the bulk.

DOI: 10.1103/PhysRevB.76.180408 PACS number(s): 75.30.Hx, 76.30.−v

Rare-earth ion doped crystals are widely used as phosphors for display, ligthing, and scintillation and also as laser and optical amplifier materials. Besides these well-known applications, they have also proved powerful for radio frequency optical processing[1] and are promising candidates for quantum information.[2,3] In these advanced fields, one takes advantage of the extremely narrow homogeneous linewidth (i.e., long coherence lifetime T_2) of some rare-earth transitions either in the optical or the radio frequency (RF) domain. For example, a homogeneous linewidth of only 0.03 Hz has been measured for a hyperfine transition of Pr^{3+} in Y_2SiO_5 using appropriate magnetic fields and RF decoupling pulses.[4] This was used to demonstrate light storage for more than one second in this compound.[2] A two-qubit logical gate,[5] and single-qubit arbitrary rotations were also demonstrated in the same crystal.[6]

A 73 Hz wide transition was observed at 1536 nm in $Er^{3+}:Y_2SiO_5$ (Er:YSO), which is the narrowest optical linewidth ever recorded in a solid.[7] This result is especially relevant for applications because of the strong development of optical fiber telecommunications around 1.5 μm. Er:YSO has already been used for high resolution spectral analysis,[1] laser stabilization,[8] and ultraslow light by coherent population oscillations,[9] and is also investigated for quantum storage.[10]

The narrow linewidth of rare-earth transitions are mainly due to the shielding of 4*f* electrons from the environment by closed 5*s* and 5*p* shells. The mechanisms which contribute to the linewidth are (i) the natural lifetime of the excited states, (ii) the rare-earth–rare-earth interactions, (iii) the coupling to phonons, and (iv) the rare-earth-host interaction mainly due to nuclear and electron-spin fluctuations of the host lattice. If one works with a rare earth having long radiative lifetime, with crystals with low rare-earth doping level and at low temperature (T=1.5 K), the first three mechanisms can be strongly suppressed. Then, the remaining process broadening the transition is the coupling between the magnetic moment of the rare-earth ions and those of the host. To reduce this contribution, hosts with no electronic moment and low average nuclear moment for all constituting elements have to be chosen. For instance, the narrowest homogeneous linewidth was observed in Er:YSO with a 10 ppm Er concentration and was obtained at 1.5 K under a high magnetic field to reduce phonon-induced Er spin flips. The 73 Hz linewidth measured this way is close to the 14 Hz limit given by the population lifetime.[8] In Ref. 8, the author suggests that the remaining difference with this limit is due to fluctuating yttrium nuclear spins through resonant flip-flop mechanisms around the Er ions. The study of this decoherence process is a complex problem since the magnetic moment of the rare-earth ions may shift the nuclear frequency of the closest host nuclei out of resonance from the nuclear frequency of bulk nuclei, giving rise to a "frozen core" effect.[11] Few studies, only performed on Pr-doped compounds, addressed this particular rare-earth-host interaction problem. Burum *et al.* studied by means of optically detected NMR the superhyperfine interactions between Pr^{3+} ions and fluorine ions in $Pr:CaF_2$.[12] Raman heterodyne experiments where a nuclear coherence created by RF fields and read out by optical techniques were performed on $Pr:LaF_3$,[13] $Pr:YAlO_3$,[14] and $Pr:Y_2SiO_5$.[15]

This frozen core effect has a direct influence on the coherence lifetime of the rare-earth ion transitions: the spin flip rate of nuclei in the frozen core is reduced since they do not experience flip-flop processes with the nuclei of the bulk material. This then reduces the magnetic field fluctuations around the rare earth and increases the transition coherence lifetimes. Direct measurements of the rare-earth-host interactions are therefore important to study decoherence. Moreover, the analysis of rare-earth-host interactions is the first step for quantum computing protocols using the spin-bus concept. Indeed, the electron spin of Er^{3+} could act as a bus qubit connected to a finite number of Y^{3+} nuclear spins playing the role of client qubits.[16]

In this paper we report the direct measurement by spin-echo experiments of superhyperfine interactions between Er^{3+} and Y^{3+} ions in the case of $Er:Y_2SiO_5$. In some spin-echo measurements, the intensity of the echo is modulated at the nuclear transition frequencies of the interacting nuclei leading to the electron spin-echo envelope modulation (ESEEM) spectroscopy.[17] These modulations allow us to determine which particular ions of the host interact with the rare earth.

In Y_2SiO_5, Er^{3+} ions lie on two crystallographic sites with

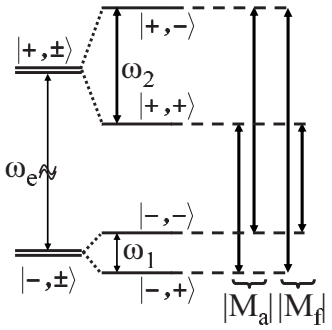

FIG. 1. Energy level diagram for an electron spin $S=1/2$ coupled with a nuclear spin $I=1/2$. For the eigenstates, $|+,-\rangle$ corresponds, for example, to m_S, m_I values of $+1/2$ and $-1/2$. $|M_a|$ ($|M_f|$) are the allowed (partially forbidden) transition matrix elements.

low-symmetry C_1. In this work, we will focus on site 1 which is the site of interest for applications.[18] In Y_2SiO_5, Er^{3+} ions can only interact with the nuclear spins of Y^{3+} ions, Si^{4+} ions, and O^{2-} ions. Y^{3+} ions have one 100% abundant isotope with a nuclear spin $I=1/2$ and a nuclear g-factor $g_n=-0.2748$. Due to their low isotopic natural abundances, contributions of ^{17}O (0.038%) and ^{29}Si (4.67%) isotopes will be negligible compared to the ones of Y^{3+} ions. As in the following we only perform experiments on Er isotopes with no nuclear spins, the spin Hamiltonian for an Er-Y pair is

$$H = \beta_e \mathbf{B}\cdot\tilde{\mathbf{g}}\cdot\mathbf{S} - \beta_n g_n \mathbf{B}\cdot\mathbf{I} + \mathbf{H}^{int}, \quad (1)$$

with β_e the electronic Bohr magneton and β_n the nuclear magneton. $\mathbf{B}$ is the external static magnetic field and $\tilde{\mathbf{g}}$ is the 3×3 g-factor matrix. $\mathbf{S}$ refers to the electronic spin of Er^{3+} ions and $\mathbf{I}$ refers to the nuclear spin of Y^{3+} ions. At helium temperature, Er^{3+} is well described by a $1/2$ electronic spin. $\mathbf{H}^{int}$ represents the interaction between the Er^{3+} ions and the host nuclei. A magnetic dipole-dipole interaction between Er and Y gives the following form for $\mathbf{H}^{int}$:

$$\mathbf{H}^{int} = \frac{\mu^{Er}\mu^{Y}}{R^3} - \frac{3(\mu^{Er}\cdot\mathbf{R})(\mu^{Y}\cdot\mathbf{R})}{R^5}, \quad (2)$$

where μ^{Er} and μ^{Y} are the electronic and nuclear magnetic dipole moments of Er and Y written as $\mu^{Er}=\beta_e\mathbf{g}\cdot\mathbf{S}$ and $\mu^{Y}=\beta_n g_n\mathbf{I}$, respectively.

Figure 1 shows the energy level diagram of an Er-Y pair corresponding to an electron spin $S=1/2$ coupled with a nuclear spin $I=1/2$.

The first part of the spin Hamiltonian of Eq. (1) (electronic Zeeman interaction) splits the fourfold degenerate levels of the pair into two doublets, $|-,\pm\rangle$ and $|+,\pm\rangle$, separated by the electronic frequency ω_e. The nuclear Zeeman interaction ($\beta_n g_n \mathbf{B}\cdot\mathbf{I}$) and the dipole-dipole interaction $\mathbf{H}^{int}$ split the two doublets into two singlets separated by the superhyperfine frequencies ω_1 and ω_2.

The crystal used in our experiments is supplied by Scientific Materials Inc. A cube of 1 mm^3 doped with 0.005 at. % of Er^{3+} ions is oriented along the three orthogonal optical extinction axes (b,D_1,D_2). Electron paramagnetic resonance (EPR) measurements were carried out using a Brüker EL-

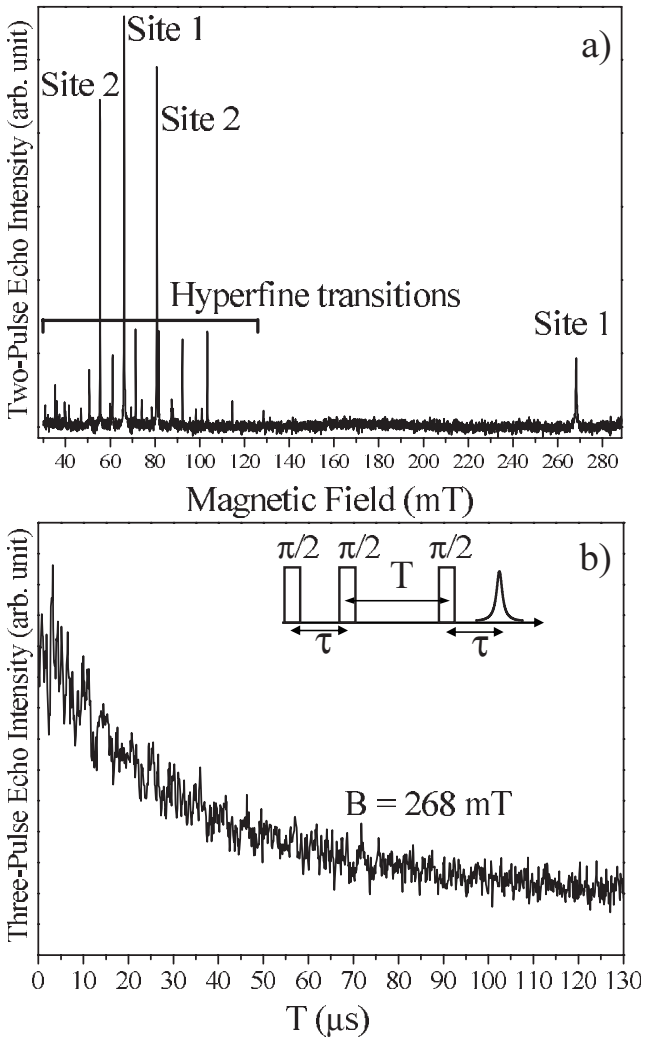

FIG. 2. (a) Field-swept Er^{3+} EDEPR spectrum at 4 K in Y_2SiO_5 collected with a two-pulse echo sequence $\pi/2-\tau-\pi-\tau-$echo with $\pi/2$ pulse length of 16 ns, and $\tau=200$ ns. The spectrum is obtained for an external magnetic field in the (b,D_1) plane oriented at 43° from the b axis. Hyperfine transitions are due to ^{167}Er. (b) Electron spin-echo decay of site 1 at 4 K with $B=268$ mT in a three-pulse experiment as a function of the time T between the second and the third pulse with the same magnetic field orientation. In three-pulse ESEEM experiments τ was set to 136 ns.

EXYS E580 pulsed EPR spectrometer in the X band at 4 K. All the experiments were performed in the (b,D_1) plane with the external magnetic field oriented at 43° from the b axis. This magnetic field orientation was chosen to avoid an overlap between the EPR spectra of sites 1 and 2 and to ascertain that only site 1 was excited by the microwave pulses.[19] To check this orientation, an echo detected EPR (EDEPR) spectrum was collected using a two-pulse echo sequence $\pi/2-\tau-\pi-\tau-$ echo while sweeping the magnetic field [Fig. 2(a)].

ESEEM experiments at 4 K performed on site 1 at a magnetic field of 268 mT are obtained by recording the echo intensity generated by a three-pulse sequence (stimulated echo sequence) $\pi/2-\tau-\pi/2-T-\pi/2-\tau-$ echo.[17,20] Two nonselective $\pi/2$ pulses, which excite all electronic transi-

tions, separated by time τ are applied and followed by a third nonselective $\pi/2$ pulse after time T. The stimulated echo is observed at time τ after the third pulse [Fig. 2(b)]. The echo intensity of the three-pulse ESEEM experiment for an Er-Y pair with a fixed time τ and a variable time T is given by[17,20]

$$I(\tau,T) = \tfrac{1}{2}[V^1 + V^2] \tag{3}$$

with

$$V^1 = 1 - \frac{k}{2}[1 - \cos(\omega_2\tau)]\{1 - \cos[\omega_1(\tau+T)]\},$$

$$V^2 = 1 - \frac{k}{2}[1 - \cos(\omega_1\tau)]\{1 - \cos[\omega_2(\tau+T)]\}. \tag{4}$$

k is called the modulation depth parameter and is linked to transition probabilities between the two allowed and the two partially forbidden electronic transitions: $k=4|M_a|^2|M_f|^2$.[21] If one of the transitions is strictly forbidden, i.e., $|M_f|=0$, no modulation appears. In the case of N interacting Y^{3+} ions, Eq. (3) becomes[21]

$$I(\tau,T) = \frac{1}{2}\left[\prod_{i=1}^{N} V_i^1 + \prod_{i=1}^{N} V_i^2\right], \tag{5}$$

with V_i^1 and V_i^2 defined by Eq. (4). Equations (3)–(5) are valid provided one can neglect the nonsecular terms of Eq. (2) proportional to S_x and S_y operators. This is the case in our system where ω_e around 10 GHz is large compared to ω_1 and ω_2 around 1 MHz.

Figure 2(b) presents the decay at 4 K of the echo amplitude as a function of the time T between the second and the third pulse. Shallow modulations are observed in the echo amplitude decay [Fig. 2(b)]. The Fourier transform (FT) spectrum [Fig. 3(a)] consists of a pattern centered around 0.56 MHz. This frequency corresponds to the nuclear frequency of Y^{3+} ions far from erbium ions [term $\beta_n g_n \mathbf{B}\cdot\mathbf{I}$ in Eq. (1)]. By considering the crystal structure and Er-Y pair distances and orientations, the pattern around this central frequency is unambiguously attributed to Y^{3+} ions around Er^{3+} ions. The position of the lines are calculated by assuming a magnetic dipole-dipole interaction [Eq. (2)]. To calculate $\mathbf{H}^{int}$, the g matrix associated to Er^{3+} ions in site 1 with respect to the three orthogonal optical extinction axes (D_1, D_2, b) was determined by a cw-EPR study.[19] The Er-Y distances and orientations are fixed by the crystallographic positions of each ion. The calculated modulation frequencies, obtained without any adjustable parameter, allow us to attribute each modulation line to a particular Y^{3+} ion. Each Er-Y pair gives two modulation lines which correspond to the frequencies ω_1 and ω_2 of Fig. 1. The intense lines are due to the nearest Y^{3+} ions [Fig. 3(a)]. The broad structure around 0.56 MHz is due to Y^{3+} ions located at distances ranging between 4 Å and 6 Å around the central Er^{3+} ion. The Y^{3+} ions at $R>6$ Å do not bring any contribution to the spectrum due to their very low modulation depth parameter values. Small modulation peaks at higher frequencies between 1.8 and 3.5 MHz are due to Si^{4+} ions.

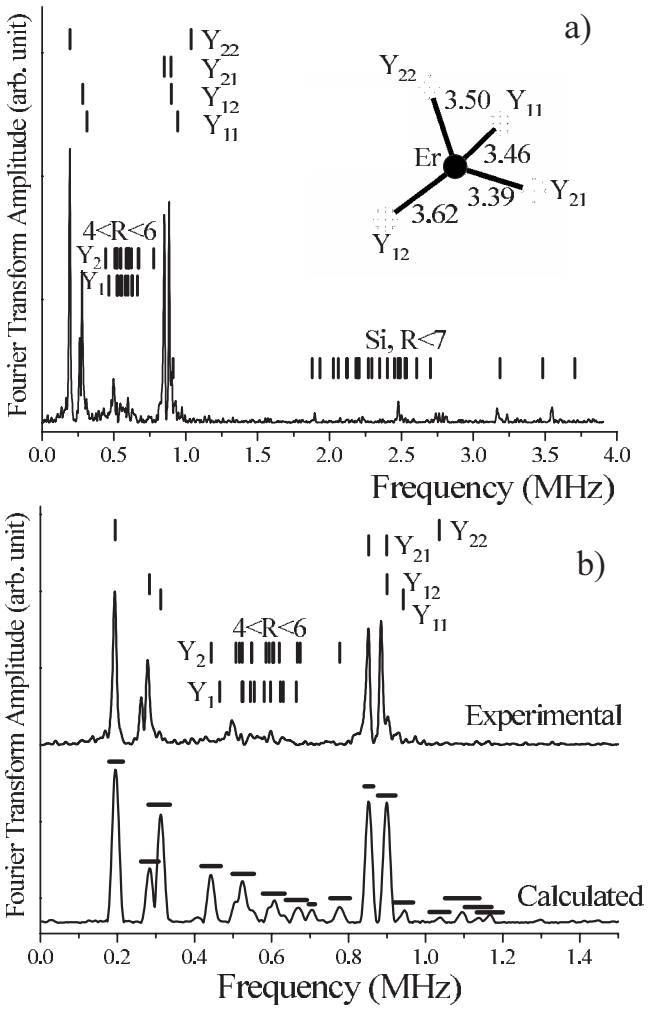

FIG. 3. (a) Magnitude-FT three-pulse ESEEM spectrum of $Er:Y_2SiO_5$. Time-domain data of Fig. 1(b) were baseline corrected by a biexponential decay, apodized by a Hamming window, and zero filled up to 2^{14} points. For Y nuclei, the first index indicates the site and the second classifies the ions by increasing distances. To obtain the calculated spectrum, lattice distances are converted to dipolar coupling using Eq. (2) and then entered into Eqs. (3)–(5). The horizontal lines in (b) represent the uncertainties on the calculated frequencies ω_1 and ω_2 (see text).

For the four closest Y^{3+} ions at $R<4$ Å, the frequency shifts from the nuclear frequency of bulk yttrium ions (0.56 MHz) are ranging from 280 kHz to 370 kHz. These detunings are much larger than the 35 Hz linewidth of yttrium NMR transitions.[22] Such detunings give rise to a frozen core effect and the Y^{3+} ions in the frozen core have a weaker effect on the homogeneous linewidth of Er^{3+} ions as they are detuned from bulk yttrium.

Figure 3(b) gathers an expanded view of the experimental spectrum in the range 0–1.4 MHz along with a calculated spectrum using Eq. (5). The uncertainties on the calculated modulation frequencies [see the horizontal lines in Fig. 3(b)] are due to an experimental accuracy of ±1° for the crystal orientation in the EPR cavity. The intensities of the main peaks are well reproduced by the calculation. Some discrepancies are observed for the broad structure around

0.56 MHz. This can be due to error in the baseline correction of the time-domain data where a biexponential decay is assumed and/or to instrumental dead time (around 88 ns) which are not taken into account in the calculated spectrum.[23]

In conclusion, rare-earth-host superhyperfine interactions in $Er:Y_2SiO_5$ were directly observed by spin-echo experiments. Well-defined temporal modulations were analyzed in terms of magnetic dipole-dipole interactions between Er^{3+} ions and particular Y^{3+} ions of the structure. This study reveals a strong frozen core effect around the Er^{3+} ions which suggests that the influence of Y^{3+} ions on the decoherence processes of erbium is weaker than what can be deduced from the resonant yttrium of the bulk. Moreover, it is a first step toward quantum computing protocols based on the spin-bus concept where an Er^{3+} ion connected to a finite number of Y^{3+} nuclear spins can constitute a local processing unit.

The authors thank K. Bencheikh, E. Baldit, and J. A. Levenson for providing the $Er:Y_2SiO_5$ sample used in this work. They also wish to thank P. Milman for useful discussions and for reading the manuscript.

*Author to whom correspondence should be addressed; olivier-guillotn@enscp.fr

[1] G. Gorju, A. Chauve, V. Crozatier, I. Lorgeré, J.-L. Le Gouët, and F. Bretenaker, J. Opt. Soc. Am. B **24**, 457 (2007).
[2] J. J. Longdell, E. Fraval, M. J. Sellars, and N. B. Manson, Phys. Rev. Lett. **95**, 063601 (2005).
[3] M. Nilsson and S. Kröll, Opt. Commun. **247**, 393 (2005).
[4] E. Fraval, M. J. Sellars, and J. J. Longdell, Phys. Rev. Lett. **95**, 030506 (2005).
[5] J. J. Longdell, M. J. Sellars, and N. B. Manson, Phys. Rev. Lett. **93**, 130503 (2004).
[6] S. Kröll (private communication).
[7] T. Böttger, Y. Sun, C. W. Thiel, and R. L. Cone, Proc. SPIE **4988**, 51 (2003).
[8] Thomas Böttger, Ph.D. thesis, Montana State University, 2002.
[9] E. Baldit, K. Bencheikh, P. Monnier, J. A. Levenson, and V. Rouget, Phys. Rev. Lett. **95**, 143601 (2005).
[10] Elisa Baldit, Ph.D. thesis, Paris XI Orsay University, 2007.
[11] R. M. Macfarlane and R. M. Shelby, *Spectroscopy of Solids Containing Rare Earth Ions*, edited by A. A. Kaplyanskii and R. M. Macfarlane (North Holland, Amsterdam, 1987), p. 51.
[12] D. P. Burum, R. M. Shelby, and R. M. Macfarlane, Phys. Rev. B **25**, 3009 (1982).
[13] M. Matsushita, A. Mutoh, and T. Kato, Phys. Rev. B **58**, 14372 (1998).
[14] L. E. Erickson, Phys. Rev. B **47**, 8734 (1993).
[15] E. Fraval, M. J. Sellars, A. Morrison, and A. Ferris, J. Lumin. **107**, 347 (2004).
[16] M. Mehring and J. Mende, Phys. Rev. A **73**, 052303 (2006).
[17] S. A. Dikanov and Y. D. Tsvetkov, *Electron Spin Echo Envelope Modulation (ESEEM) Spectroscopy* (CRC Press, Boca Raton, FL, 1992).
[18] T. Böttger, C. W. Thiel, Y. Sun, and R. L. Cone, Phys. Rev. B **73**, 075101 (2006).
[19] O. Guillot-Noël, P. Goldner, Y. Le Du, E. Baldit, P. Monnier, and K. Bencheikh, Phys. Rev. B **74**, 214409 (2006).
[20] A. Schweiger and G. Jeschke, *Principles of Pulse Electron Paramagnetic Resonance* (Oxford University Press, Oxford, 2001).
[21] W. B. Mims, Phys. Rev. B **6**, 3543 (1972).
[22] R. Dupree and M. E. Smith, Chem. Phys. Lett. **148**, 41 (1988).
[23] S. Van Doorslaer, G. A. Sierra, and A. Schweiger, J. Magn. Reson. **136**, 152 (1999).